A GRAPHICAL REVIEW OF NOISE-INSTABILITY CHARACTERIZATION IN ELECTRONIC SYSTEMS

Juan José González de la Rosa
Univ. Cádiz. Electronics Area, EPSA. Ramón Puyol S/N. E-11202-Algeciras-Spain

Isidro Lloret Galiana
Univ. Cádiz. Dpt. Computer Science, EPSA. Ramón Puyol S/N. E-11202-Algeciras-Spain

Carlos García Puntonet
Univ. Granada. Dept. ATC, ESII. Periodista Daniel Saucedo. E-18071-Granada-Spain

Víctor Pallarés López
Univ. Córdoba. Dept. Electronics, Campus Rabanales. A. Einstein. C-2. E-14071. Córdoba. Spain

Keywords: Allan deviation, enveloping curves, frequency stability, GPS-receiver, noise processes, traceable calibration.

Abstract: A thorough study of the noise processes characterization is made with simulated data by means of our non-classical estimators. Individual and hybrid noise sequences, previously generated by seed functions, have been used to obtain a set of characterization graphs identifying the noise type by mean of the enveloping curve. It is also shown the case of a hidden noise. An real test situation is presented which involves a traceable characterization via a GPS receiver.

1 INTRODUCTION

Noise affects short-term stability of clocks and oscillators of systems in a broad range of technical fields like communications, instrumentation and medicine. The relationship between the causes and the different noise processes is continuously being reviewed (Vig, 2001). Random oscillator instabilities are linked to the environment (temperature changes, vibrations, shock and electromagnetic fields) and to the *guts* of the electronics components (thermal noise, internal irregularities in the xtal and the semiconductor devices, and surface imperfections).

Numerous works have provided the users with useful analytical tools with the aim of getting the completeness of the calibration procedure (Allan, 1987), (Rutman and Walls, 1991). Multivariance analysis allows getting higher measurement accuracy (Vernotte, 1993) in estimating the uncertainties in order to better distinguish the different types of noises.

In this work we have summarized the subject to have an unified practical frame, understandable in multidisciplinary engineering projects. An analysis of the noise processes is performed to provide an easy-going review of short term instability characterization, by analyzing the slopes of the AVAR[1] and MVAR[2] in the log-log curves. Noise time series have been simulated and estimators of the variances have been programmed with the aim of having a thorough vision of the time-domain slopes when compared to former works: (Howe et al., 1999), (Allan, 1987), (Rutman and Walls, 1991), (Vernotte, 1993), (Vig, 2001).

The paper is structured as follows: in Section 2 we review the oscillators independent noise processes and the methods used to identify them; Section 3 shows the simulation results concerning time-domain stability characterization. The concept of enveloping curve is introduced herein withe the objective of characterizing the effects of different simultaneous noise processes. A real case of short-term characterization procedure and its associated conclusions are presented in Section 4. In this section, we consider a precision function generator as device under test in a GPS-traceable characterization.

2 CLASSICAL NOISE MODELS

It is a customary situation to deal with unperfect signals which contain additive noise. The instantaneous

[1] Allan variance or two-sample Allan variance

[2] Modified Allan variance

José González de la Rosa J., Lloret Galiana I., García Puntonet C. and Pallarés López V. (2005).
A GRAPHICAL REVIEW OF NOISE-INSTABILITY CHARACTERIZATION IN ELECTRONIC SYSTEMS.
In *Proceedings of the Second International Conference on Informatics in Control, Automation and Robotics - Signal Processing, Systems Modeling and Control*, pages 310-315
DOI: 10.5220/0001154903100315

output voltage of an oscillator can be expressed as:

$$v(t) = [V_o + \varepsilon(t)]\, sin\,[2\pi\nu_0 t + \phi(t)]\,, \qquad (1)$$

where V_o is the nominal peak voltage amplitude, $\varepsilon(t)$ is the deviation from the nominal amplitude, ν_0 is the name-plate frequency, and $\phi(t)$ is the phase deviation from the ideal phase $2\pi\nu_0 t$. Changes in the peak value of the signal is the amplitude instability. Fluctuations in the zero crossings of the voltage is the phase instability. The so-called frequency instability is depicted by the fluctuations in the period of the voltage. The situation is depicted in figure 1[3].

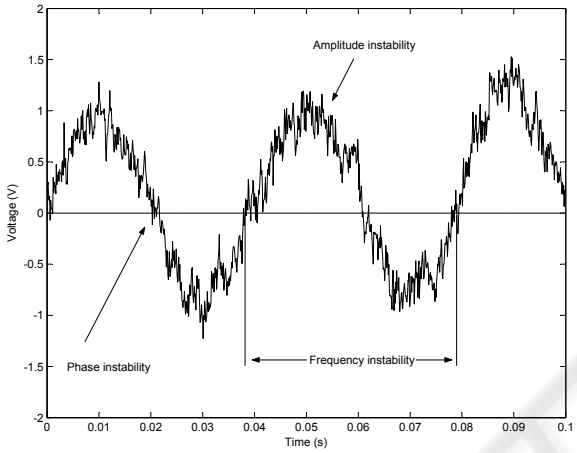

Figure 1: Simulated types of instabilities in a 25 Hz sinusoidal output with additive noise. The noise process has a power spectral density proportional to the inverse of the frequency (flicker phase modulation).

The impacts of oscillator noise and the causes of short term instabilities have been described in many research works and tutorials like (Howe et al., 1999), (Vig, 2001) and (Sullivan et al., 1990). The short-term stability measures most frequently found on oscillator specification sheets is the two-sample deviation, also called Allan deviation, $\sigma_y^2(\tau)$.

Classical variance in non-stationary noise processes don't converge to concrete values. It diverges for some noise processes, such as random walk, i.e., the variance increases with increasing number of data points. This is the reason whereby non-classical statistics are used to characterize short term instability.

AVAR and MVAR have proven their adequacy in characterizing frequency phase and instabilities. These easy-to-compute variances converge for all noise processes observed in precision frequency sources, have a straightforward relationship to power law spectral density of noise processes, and are faster and more accurate in than the FFT (Lesage and Ayi, 1984).

The estimates of AVAR and MVAR for a given calibration time τ for a m-data series of phase differences, x, are given by equations 2 and 3, (Greenhall, 1988):

$$AVAR \equiv \sigma_y^2(\tau, m) = \frac{1}{2(m-1)} \sum_{j=2}^{m} \left(\overline{y}_j - \overline{y}_{j-1}\right)^2 = \frac{1}{2\tau^2(m-1)} \sum_{j=2}^{m} \left[\Delta_\tau^2 x(j\tau)\right]^2 \qquad (2)$$

$$MVAR \equiv \frac{1}{2\tau^2} \langle \Delta_\tau^2 \overline{x} \rangle^2, \qquad (3)$$

where the bar over x denotes the average in the time interval τ (averaging time), and $\Delta_\tau^2 x = x_{i+2} - 2x_{i+1} + x_i$, is the so called second difference of x. The fractional frequency deviation is the relative phase difference in an interval τ. It is defined by equation 4:

$$\overline{y} = \frac{1}{\tau} \int_{t-\tau}^{t} y(s)ds = \frac{x(t) - x(t-\tau)}{\tau} = \frac{\Delta_\tau x(t)}{\tau}. \qquad (4)$$

Non-classical statistics estimators, defined above, in equations 2 and 3, for non-stationary series characterization, give an average dispersion of the fractional frequency deviation due to the noise processes coupled to the oscillator. As a consequence time domain instability (two-sample variance) is related to the noise spectral density via (Rutman and Walls, 1991):

$$\sigma_y^2(\tau) = \frac{2}{(\pi\nu_0\tau)^2} \int_0^{f_h} S_\phi(f) sin^4(\pi f \tau) df, \qquad (5)$$

where ν_0 is the carrier frequency and f is the Fourier frequency (the variable), and f_h is the band-width of the measurement system. $S_\phi(f)$ is the spectral density of phase deviations, which is in turn related to the spectral density of fractional frequency deviations by(Rutman and Walls, 1991):

$$S_\phi(f) = \frac{\nu_0^2}{f^2} S_y(f), \qquad (6)$$

The classical power-law noise model is a sum of the five common spectral densities. The model can be described by the one-sided phase spectral density $S_\phi(f)$ via (IEEE, 1988), (Greenhall, 1988):

$$S_\phi(f) = \frac{\nu_0^2}{f^2} \sum_{\alpha=-2}^{2} h_\alpha f^\alpha = \nu_0^2 \sum_{\beta=0}^{4} h_\beta f^\beta, \qquad (7)$$

for $0 \leq f \leq f_h$. Where, again, f_h is the high-frequency cut-off of the measurement system (the

[3]A similar example was provided by Prof. Eva Ferre-Pikal (Univ. of Wyoming) and used by John R. Vig in (Vig, 2001).

Table 1: Noise processes characterized by the time and frequency domain slopes. Up to bottom: random walk frequency modulation, flicker frequency modulation, white frequency modulation, flicker phase modulation, white phase modulation.

		AVAR	MVAR
$S_y(f)$	$S_\phi(f)$	$\sigma_y(\tau) \sim \lvert\tau\rvert^{\frac{\mu}{2}}$	$\sigma_y(\tau) \sim \lvert\tau\rvert^{\mu'}$
α	$\beta = \alpha - 2$	$\frac{\mu}{2}$	μ'
-2	-4	0.5	$1\ (0.5)$
-1	-3	0	$0\ (0)$
0	-2	-0.5	$-1\ (-0.5)$
1	-1	-1	$-2\ (-1)$
2	0	-1	$-3\ (-1.5)$

band-width); h_α and h_β are constants which represent, respectively, the independent characteristic models of oscillator frequency and phase noise (Allan, 1987), (IEEE, 1988), (Greenhall, 1988).

For integer values (the most common case) we have the following approximate expression:

$$\sigma_y(\tau) \sim \tau^{\mu/2}, \tag{8}$$

where $\mu = -\alpha - 1$, for $-3 \leq \alpha \leq 1$; and $\mu \approx -2$ for $\alpha \geq 1$. In the case of the modified Allan variance, the time-domain instability can be approximated via:

$$Mod\sigma_y(\tau) \sim \tau^{\mu'} \tag{9}$$

Hereinafter we use expressions 8 and 9 for analyzing noise in these work.

3 TIME DOMAIN STABILITY CHARACTERIZATION CURVES

Equations 8 and 9 are used to make the graphical representation of $\sigma_y(\tau)$ vs. τ, and lets us infer the noise processes which causes frequency instability by means of measuring the slope in a log-log graph (Rutman and Walls, 1991), (Wei, 1997). These functional characteristics of the independent noise processes are widely used in modelling frequency instability of oscillators. Table 1 shows the experimental criteria adopted in the main references. In the second column or MVAR we have picked up two different criteria according to the references (Rutman and Walls, 1991) and (Lesage and Ayi, 1984), respectively. We have kept the notation in the works (Rutman and Walls, 1991) and (Lesage and Ayi, 1984) for $\mu/2$ and μ', respectively.

The five noise processes have been modelled and VAR and MVAR have been calculated. Hereinafter we show the simulation results of the time-series and their associated VAR and MVAR graphs. From this simulations we adopt the criteria depicted in the second column of MVAR in table 1. Figures 2-6 show the simulations results. Each data sequence contains 4096 points for a time resolution of $\tau = 10^{-4}\ s$. Allan deviation curves have been depicted for averaging times $\tau = n \times \tau_0$, with $n \in [1, 500]$.

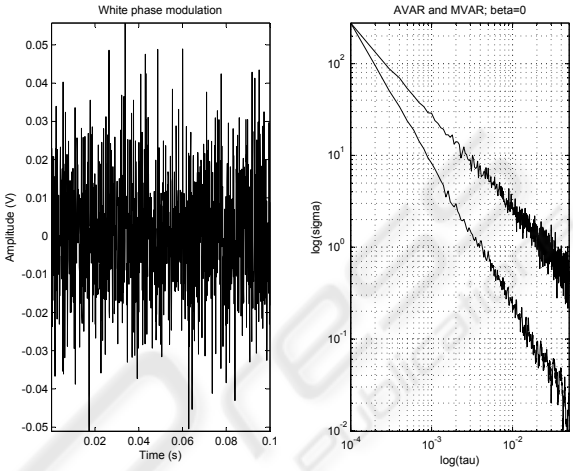

Figure 2: Characterization of a noise process corresponding to $\beta = 0$.

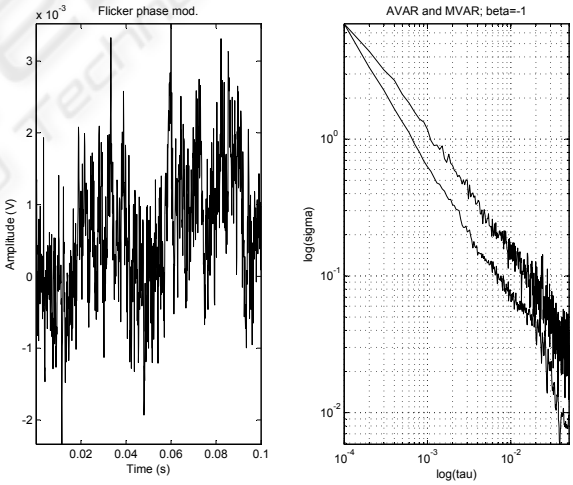

Figure 3: Characterization of a noise process corresponding to $\beta = -1$.

In many practical situations two or more noise processes simultaneously affect clocks performance. In this cases instability of the device under test is explained away through the behaviour of the upper enveloping curve. If the individual variance curves cross each other, it is possible to see the slope changes in the variance curve, for a time-series which includes several types of noise(Vernotte, 1993). This situation is shown in figures 7 and 8.

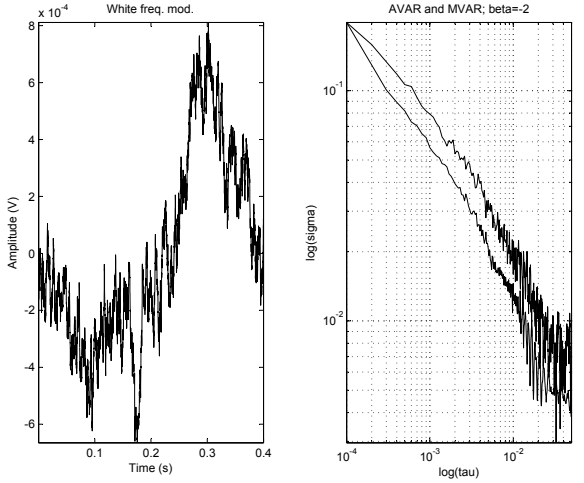

Figure 4: Characterization of a noise process corresponding to $\beta = -2$.

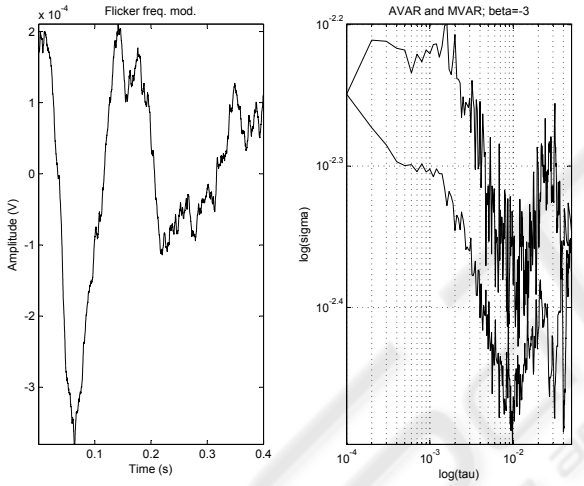

Figure 5: Characterization of a noise process corresponding to $\beta = -3$.

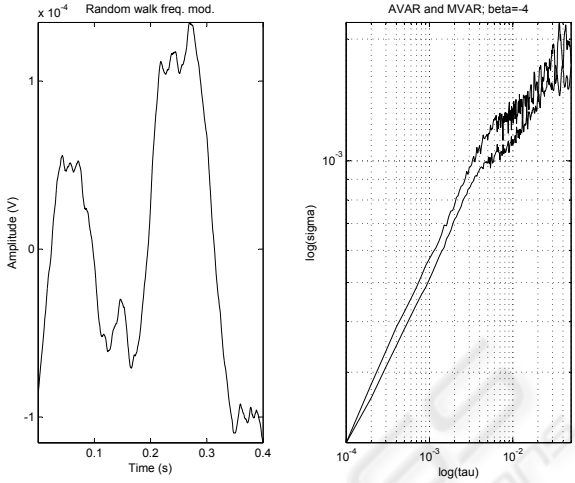

Figure 6: Characterization of a noise process corresponding to $\beta = -4$.

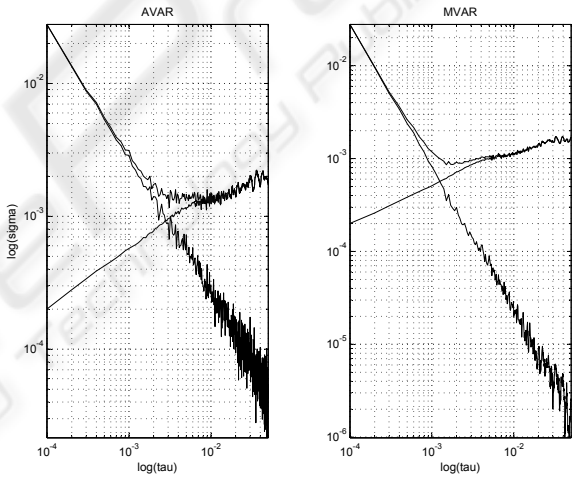

Figure 7: Noise processes corresponding to $\beta = 0$ and $\beta = -4$. Situation of changing slope.

In figure 7, the individual variance curves cross. So the enveloping curve characterizes the short-term instability. By the contrary, in figure 8 the $\beta = 0$ noise processes has a variance greater than the $\beta = -4$ perturbation. In this case the enveloping curve is the first (upper) AVAR curve.

4 EXPERIMENTAL RESULTS AND CONCLUSIONS

A high resolution function generator is chosen as device under test. It is set up to deliver a 1.1 Hz TTL signal. The experimental arrangement is depicted in figure 9. The measurement system comprises a TIC[4], a GPS receiver and the frequency source under test. These instruments have been connected via GPIB to the computer. Data points are captured every $1\ s$.

Time interval counters (TICs) and GPS receivers are widely used in traceable frequency calibrations. A transfer standard receives a signal that has a cesium oscillator as source (Lombardi, 1999). This signal delivers a cesium derived frequency to the user, who is benefited as not all laboratories can afford a cesium (Lombardi, 1996). These instruments differ in specifications and details regarding the time base, the main gate and the counting assembly. Furthermore, manufacturers tend to omit the conditions under these spec-

[4]Time Interval Counter

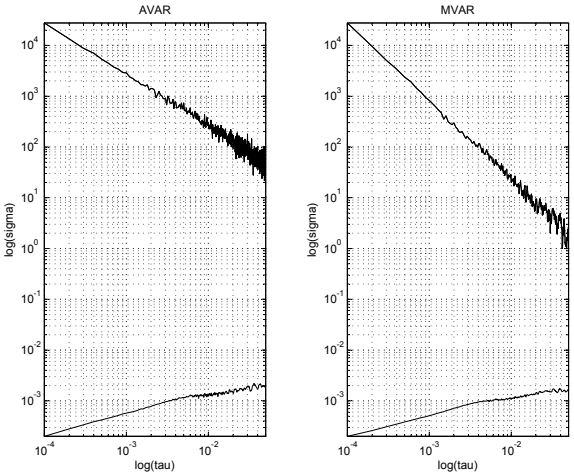

Figure 8: Noise processes corresponding to $\beta = 0$ and $\beta = -4$. The upper noise process is the enveloping curve.

ifications have been provided or measured.

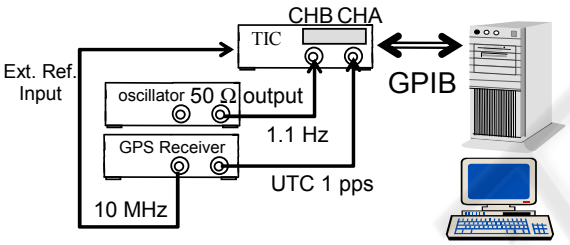

Figure 9: Experimental arrangement.

Figure 10 shows the signals involved in the measurement process. Each measurement cycle corresponds to 1 s. The bottom graph corresponds to the instantaneous phase-deviation series, which comprises $m = 898$ data. These data are the result of filtering the spiky time-series of phase differences, and are used to perform the calibration. These data are supposed to be corrupted by white noise, with a rectangular probability density function. This is corroborated later by means of AVAR and MVAR.

The ratio of the classical variance (VAR) to the Allan variance (AVAR) provides a primary test for white noise. This quantity (0.672) is less than $1 + 1/\sqrt{m} \simeq 1.033$; thus it is probably safe to assume that the data set is dominated by white noise, and the classical statistical approach can safely be used. Failure of the test does not necessarily indicate the presence of non-white noise (Fluke, 1994).

A slope test (based in AVAR and MVAR curves) has been developed to confirm the presence of white noise. AVAR and MVAR curves are depicted in figure 11.

Measures of the slopes over the log-log graphs in

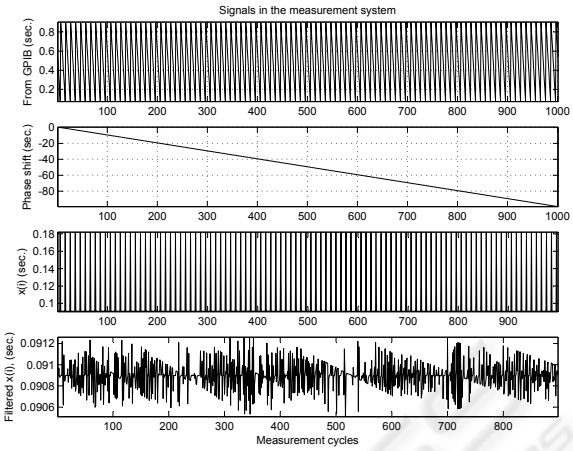

Figure 10: Signals in the measurement chain. From top to bottom: original data from the TIC and the GPIB interface, accumulated phase shift, spiky phase differences, filtered phase differences.

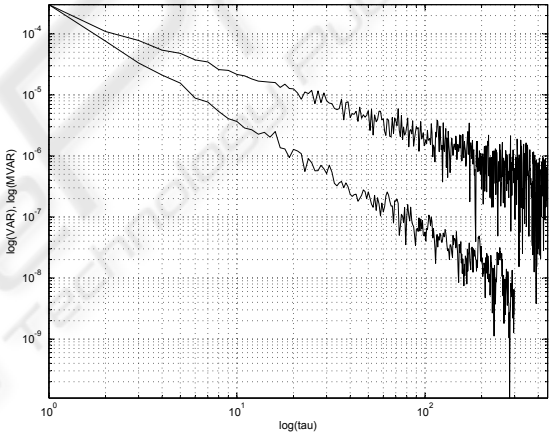

Figure 11: AVAR (upper) and MVAR (lower) log-log curves. The final calibration period is $\tau = 500 \times \tau_0$ for $\tau_0 = 1$ s.

figure 11 offer the results -1 and -1.5 for $log(AVAR)$ vs. $log(\tau)$, and $log(MVAR)$ vs. $log(\tau)$, respectively; which indicate that a white phase modulation process is coupled to the frequency source under test (see table 1).

ACKNOWLEDGEMENT

The authors would like to thank the *Spanish Ministry of Education and Science* for funding the project DPI2003-00878 which involves noise processes modelling and time-frequency calibration.

REFERENCES

Allan, D. (1987). Time and frequency (time-domain) characterization, estimation, and prediction of precision clocks and oscillators. *IEEE Transactions on Ultrasonics, Ferroelectrics, and Frequency Control*, 34(752):647–654.

Fluke (1994). *Calibration: Philosophy in Practice*. Fluke, 2 edition.

Greenhall, C. (1988). Frequency stability review. TDA progress report. Technical Report 42-88, Communications Systems Research Section.

Howe, D., Allan, D., and Barnes, J. (1999). Properties of oscillator signals and measurement methods. Technical report, Time and Frequency Division. National Institute of Standards and Technnology.

IEEE (1988). IEEE standard definitions of physical quantities for fundamental frequency and time metrology. Technical Report IEEE Std 1139-1988, The Institute of Electrical and Electronics Engineers, Inc., 345 East 47th Street, New York, 10017, USA.

Lesage, P. and Ayi, T. (1984). Characterisation or frequency stability: Analysis of the modified allan variance and properties of its estimate. *IEEE Trans. on Instrumentation and Measurement*, IM-33(4):332–336.

Lombardi, M. (1996). An introduction to frequency calibrations. *The International Journal of Metrology*, (January/February 1996).

Lombardi, M. (1999). Traceability in time and frequency metrology. *The International Journal of Metrology*, (September/October 1999).

Rutman, J. and Walls, F. (1991). Characterization of frequency stability in precision frequency sources. *Proc. IEEE*, 79(7):952–960.

Sullivan, D., Allan, D., Howe, D., and Walls, F. (1990). Characterization of clocks and oscillators. *NIST Tech Note*, 868(1337). BIN: 868.

Vernotte (1993). Oscillator noise analysis: Multivariance measurement. *IEEE Transactions on Instrumentation and Measurement*, 42(2):342–350.

Vig, J. R. (2001). *A Tutorial For Frequency Control and Timing Applications*.

Wei, G. (1997). Estimations of frequency and its drift rate. *IEEE Trans. on Instrumentation and Measurement*, 46(1):79–82.